Thermal spin dynamics of yttrium iron garnet

Barker, Joseph; Bauer, Gerrit E.W.

DOI
10.1103/PhysRevLett.117.217201

Publication date
2016

Document Version
Final published version

Published in
Physical Review Letters

Thermal Spin Dynamics of Yttrium Iron Garnet

Joseph Barker[1] and Gerrit E. W. Bauer[1,2,3]
[1]Institute for Materials Research, Tohoku University, Sendai 980-8577, Japan
[2]WPI-AIMR, Tohoku University, Sendai 980-8577, Japan
[3]Kavli Institute of NanoScience, Delft University of Technology, Lorentzweg 1, 2628 CJ Delft, The Netherlands
(Received 12 July 2016; revised manuscript received 25 September 2016; published 14 November 2016)

The magnetic insulator yttrium iron garnet can be grown with near perfection and is therefore and ideal conduit for spin currents. It is a complex material with 20 magnetic moments in the unit cell. In spite of being a ferrimagnet, YIG is almost always modeled as a simple ferromagnet with a single spin wave mode. We use the method of atomistic spin dynamics to study the temperature evolution of the full spin wave spectrum, in quantitative agreement with neutron scattering experiments. The antiferromagnetic or optical mode is found to suppress the spin Seebeck effect at room temperature and beyond due to thermally pumped spin currents with opposite polarization to the ferromagnetic mode.

DOI: 10.1103/PhysRevLett.117.217201

I. Introduction.—Spin transport in magnetic insulators has attracted much interest since the experimental demonstration of the Spin Seebeck effect (SSE) [1]. The field of study is broadly termed spin caloritronics and encompasses the coupling between spin, charge, and heat currents [2]. Typical experimental setups consist of bilayers made of a ferrimagnetic insulator coated with a thin metallic film possessing a large spin Hall angle. Of special interest is the ferrimagnetic insulator yttrium iron garnet (YIG) due to its very low damping, $\alpha \approx 10^{-5}$, and, therefore, long-lived spin waves [3,4]. The magnetism is carried by localized Fe moments in 8 tetrahedral (minority) and 12 octahedral (majority) oxygen cages per unit cell, with an antiparallel ferrimagnetic state between the two coordinations. However, most recent theories and experiments treat YIG as a *ferromagnet* (FM) with a single, parabolic spin wave mode [5,6], simply because the influence of YIG's complex electronic and magnetic structure on spin transport is not known. Ohnuma *et al.* [7] introduced a simple two-mode model to describe the basic aspects of ferrimagnetic dynamics, but its spectrum bears little resemblance to that of YIG [3]. In this Letter we show that the frequencies and linewidths of spin waves in YIG are strongly temperature dependent. We find that at room temperature higher-frequency spin wave modes are significantly occupied. Optical modes with opposite polarization to the acoustic mode turn out to have a disproportionate effect on spin transport and must be taken into account when modeling or interpreting, for example, the spin Seebeck effect.

Experimentally, techniques such as Brillouin light scattering give access to the long wavelength, GHz frequency, dipole spin waves [8]. Studying the THz frequency "exchange" spin wave modes requires expensive inelastic neutron scattering experiments [9]. The role of the high-frequency "thermal" magnons remains poorly understood, despite their importance in interpreting recent experiments [10–14]. The present theory focuses on interface-dominated transport, not addressing the possibly dominant contribution of subthermal magnons to the spin Seebeck effect in thick YIG layers [10,15,16]. Since spin wave spectra are material specific, improving the understanding of general characteristics could aid in the selection of materials to progress towards applications such as sensing and heat scavenging [17,18].

II. Atomistic model.—YIG is an insulator with a large electronic band gap. The Fe^{3+} ion d shells are half filled with a spin value of $S = 5/2$ and can be modeled with the Heisenberg Hamiltonian:

$$\mathcal{H} = -\frac{1}{2}\sum_{ij} J_{ij}\mathbf{S}_i \cdot \mathbf{S}_j - \sum_i \mu_{s,i}\mathbf{B}\cdot\mathbf{S}_i. \qquad (1)$$

Here, J_{ij} is the isotropic exchange energy between (normalized) spins with $|\mathbf{S}_i| = 1$, where the indices i, j enumerate sites on the YIG crystal lattice. The Fe^{3+} magnetic moment is $\mu_s = g\sqrt{S(S+1)}\mu_B = 5.96\mu_B$ (μ_B is the Bohr magneton). An external field $B_z = 0.01$ T defines the spin quantization (z) axis. The crystal magnetic anisotropy and dipolar interaction of YIG are negligibly small compared to THz frequencies of thermal spin waves and are disregarded here. Neutron scattering [9] indicates that nearest-neighbor exchange dominates and we adopt $J_{ad} = -9.60 \times 10^{-21}$ J, $J_{dd} = -3.24 \times 10^{-21}$ J, and $J_{aa} = -0.92 \times 10^{-21}$ J [3], where the subscripts refer to the majority (d) and minority (a) spins. Since all couplings are antiferromagnetic, the competition between inter- and intrasublattice exchange can cause frustration. However, the dominant intersublattice J_{ad} renders the perfectly anticollinear ground state stable. By Metropolis Monte Carlo calculations [19], we compute the magnetization $\mathbf{m} = (1/N_a)\sum_i \mathbf{S}_{a,i} + (1/N_d)\sum_i \mathbf{S}_{d,i}$ as a function of temperature and find a Curie temperature of 520 K, close to the experimental value of 559 K [20] and in agreement

with other calculations [21]. Throughout this work we address a bulk system by periodic boundary conditions for a supercell of repeated unit cells.

The spin wave spectrum can be obtained by diagonalizing the Hamiltonian Eq. (1) [3], but the inclusion of nonlinear effects such magnon-magnon interactions, thermal noise, and damping requires a different approach. At finite temperatures, the spin moments fluctuate around the local equilibrium state. The exchange coupling correlates the motion of all moments, giving rise to collective spin waves. The dynamical structure factor (or spin wave power spectrum) as measured by inelastic neutron scattering is the Fourier transform of spatiotemporal spin-spin correlation functions. Here, we compute the local spin dynamics, and from them, the structure factor, thereby avoiding a magnon ansatz. Therefore, magnon interactions to the highest order allowed by the symmetries of the Hamiltonian are implicitly included. However, we are cannot specify the nature and consequences of magnon scattering processes as is possible in a many-magnon basis expansion.

The spin dynamics is described by the atomistic Landau-Lifshitz-Gilbert equation based on the Hamiltonian Eq. (1):

$$\frac{\partial \mathbf{S}_i}{\partial t} = -\frac{|\gamma|}{(1+\lambda^2)\mu_{s,i}}(\mathbf{S}_i \times \mathbf{H}_i + \lambda \mathbf{S}_i \times \mathbf{S}_i \times \mathbf{H}_i). \quad (2)$$

The local effective field is $\mathbf{H}_i = \boldsymbol{\xi}_i - \partial\mathcal{H}/\partial\mathbf{S}_i$ where ξ_i is a stochastic term with

$$\langle \xi_i(t) \rangle = 0; \quad \langle \xi_i(t)\xi_j(t') \rangle = \delta_{ij}\delta(t-t')2\lambda\mu_s k_B T/\gamma, \quad (3)$$

where $\langle \cdots \rangle$ denotes the statistical time average. The electronic gyromagnetic ratio is $\gamma = 1.76\times10^{11}$ rad s^{-1} T^{-1}. The measured Gilbert damping α of ferrimagnets is a combination of the damping parameters of the sublattices. According to the Wangsness formula, $\alpha = (\lambda_a M_a + \lambda_d M_d)/(M_d - M_a)$ [22]. Here we use the damping parameter $\lambda = \lambda_a = \lambda_d = 2\times10^{-5}$ giving $\alpha = 10^{-4}$, which is a typical (although not record) value. We solve the stochastic Langevin equation (2) with the Heun method, using a time step of $\Delta t = 0.1$ fs. The low damping requires careful equilibration. We first use a Metropolis Monte Carlo algorithm to converge to the equilibrium magnetization. We then integrate the Landau-Lifshitz-Gilbert equation dynamically for 1 ns, which is sufficient to achieve a steady state regime in the presence of noise. Finally, the data collected for 0.5 ns are Fourier transformed from space and time to frequency and momentum to distill the spectral information.

In our classical equilibrium formalism the thermal noise is white, and through equipartition the system obeys Rayleigh-Jeans rather than Planck statistics for magnons. Possible quantum effects at low temperatures and high energies are disregarded in our method. However, at elevated temperatures quantum effects are suppressed by inelastic scattering processes, and classical spin models can be expected to agree well with experiments.

The spin wave spectrum is revealed in terms of structures in the space-time Fourier transform of the spin fluctuations. The Fourier representation of the spin dynamics reads

$$\mathcal{S}_k(\mathbf{q},\omega) = \frac{1}{\sqrt{2\pi}}\frac{1}{N_c}\sum_{n=1}^{N_c}\sum_{\mathbf{r}} e^{i\mathbf{q}\cdot(\mathbf{r}-\mathbf{p}_n)}\int_{-\infty}^{+\infty} e^{i\omega t} S_{k,n}(\mathbf{r},t)dt, \quad (4)$$

where $\mathbf{p}_n$ is the position of the nth spin (of a total of $N_c = 20$) in the unit cell and $k = x, y, z$. The q-space resolution is determined by the system size of $64\times64\times64$ unit cells (5 242 880 spins).

The thermal spin motive force is proportional to the transverse dynamical susceptibility or equal-time spin correlation function [5], which is proportional to the correlation function $\langle \dot{S}_{y,i}(0)S_{x,i}(0) - \dot{S}_{x,i}(0)S_{y,i}(0)\rangle$ at the interface. In perturbation theory this is equivalent to the wave vector and frequency integral of the power spectrum $\langle \omega\mathcal{S}_x(\mathbf{q},\omega)\mathcal{S}_y^*(\mathbf{q},\omega)\rangle - \langle \omega\mathcal{S}_y(\mathbf{q},\omega)\mathcal{S}_x^*(\mathbf{q},\omega)\rangle$ of the bulk ferromagnet. This correlation function is the Stokes parameter $V = -2\mathrm{Im}(\mathcal{S}_x\mathcal{S}_y^*)$, and the sign identifies the polarization of the eigenvectors [23]. The + polarization label implies a counterclockwise precessional motion with respect to an applied field, i.e., the precession direction of an electron spin under resonance.

III. Spin wave spectrum.—In Fig. 1 we display the calculated spin wave spectra for different temperatures. The coloring indicates the polarization of the modes. Red modes have the + polarization, while the blue modes precess in the opposite direction. The latter (optical) modes are energetically costly due to the strong exchange field between the two sublattices, so they emerge only at frequencies at and above the exchange splitting.

At the lowest temperature considered (1 K), the amplitude of the excitations (or number of magnons) is small and magnon interactions are very weak. The calculated spectrum therefore agrees well with the linearized spin wave theory [3]. The following discussion is focused on the two nearly rigidly shifted parabolic modes with opposite polarization. The lowest frequency mode is the ferromagneticlike acoustic mode. The second mode is blueshifted by a spin wave gap caused by the exchange field between the two sublattices, $\Delta = 3J_{ad}\langle S_{z,a}\rangle - 2J_{ad}\langle S_{z,d}\rangle \approx 10$ THz, and is the optical, antiferromagneticlike mode between the two sublattices. We observe 5 additional flat modes in the 5 and 10 THz range that are thermally excited at room temperature. Since their mass is very high, they are expected to only weakly contribute to spin transport.

Thermal fluctuations reduce the magnetic order $\langle S_{z,a}\rangle$, $\langle S_{z,d}\rangle$ and thereby the exchange field Δ, as observed in Fig. 1. Our calculations agree very well with neutron

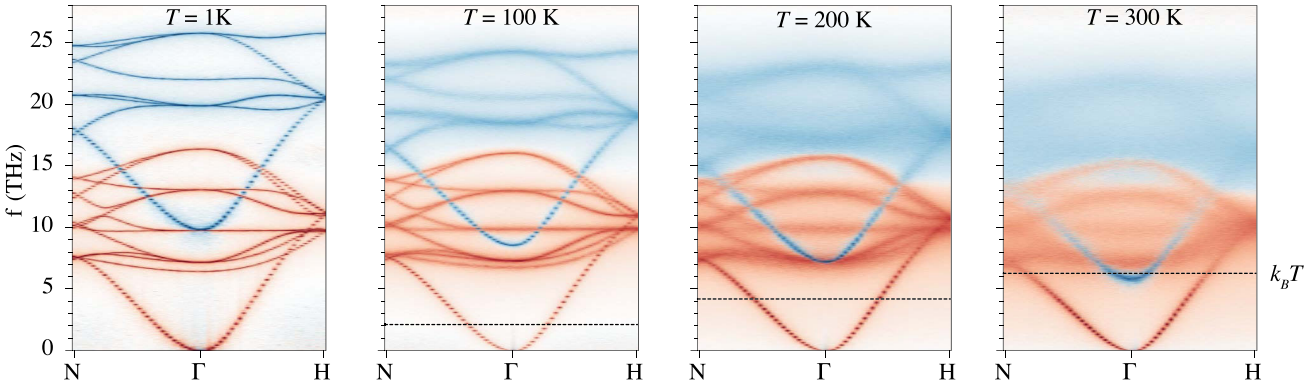

FIG. 1. YIG spin wave spectrum as calculated for different temperatures. The dashed lines mark $2\pi\hbar f = k_BT$. The red (blue) coloring denotes the + (−) mode polarization relative to the magnetization direction.

scattering experiments [9] (Fig. 2). We emphasize that our exchange constants J_{ij} are not temperature dependent—the effect is caused by statistical mechanics alone. Below $\hbar\omega = k_BT$ (dashed line), spin wave modes are thermally occupied. The occupation above this line is small and technically governed by quantum statistics, but unimportant for (near to) equilibrium properties. Far below room temperature, only the ferromagneticlike acoustic mode is significantly occupied and the use of a single parabolic spin wave model is justified. However, at room temperature and above, this approach breaks down and the effects reported here must be taken into account in order to understand the properties of YIG.

Our method allows a comprehensive treatment of the nonlinear thermodynamics from low temperatures up to the magnetic phase transition. The magnon ansatz often used to describe spin dynamics is based on the Holstein-Primakoff transformation expanded to low order in the number of magnons. A larger number of thermally excited magnons initially can be captured by magnon-magnon interactions.

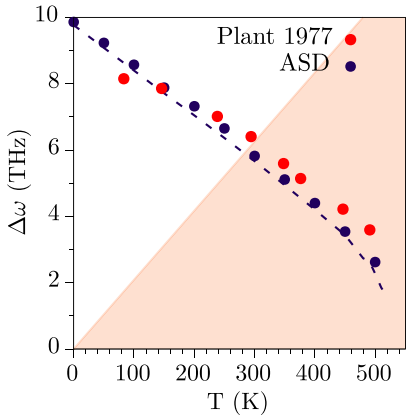

FIG. 2. Temperature dependence of the spin wave gap. Blue circles are the calculations in this work, red points are the neutron scattering data of Plant [9]. The shaded area marks $\hbar\omega < k_BT$. The dashed line is the reduction in exchange field due to spin fluctuation.

These reduce the magnon lifetime as reflected by an increased broadening of the spectral function. We confirmed this is not a result of poor statistical averaging by comparing the linewidths for 0.1 and 0.5 ns of data, finding quantitatively similar results. When the broadening becomes larger than the spin wave energy splittings, the magnon concept breaks down completely. This picture is illustrated by Fig. 1, in which we observe that with increasing temperature the flat modes completely melt into an incoherent background that can no longer be interpreted in terms of spin waves. However, the coherence of the fundamental acoustic and optical modes turns out to be remarkably robust against thermal fluctuations: the linewidths as well as the parabolic curvature, a metric of spin wave stiffness, hardly change with temperature. Our formalism can provide information about individual local moment fluctuations irrespective of the coherence of the spin wave excitations, which can be used to shed light onto this behavior. In Fig. 3 we plot the site-resolved contributions to the power spectrum. We clearly see that the fundamental acoustic and optic modes are homogeneously spread over the unit cell, while the other modes are strongly localized on one of the local moments that are consequently coupled by the small J_{aa} and J_{dd} exchange constants. The spin waves with a flat dispersion are slack and susceptible to thermal agitation. This is a form of dynamic localization which is unrelated to “Anderson" localization in disordered systems.

The resilience of both fundamental modes agrees with observations [24] but appears to contradict common wisdom that the spin wave stiffness decreases linearly with temperature [25]. The reason for the anomalous behavior of YIG has not been well understood, especially in the higher temperature regime where the optical magnons become involved [3]. The present results indicate that the decoupling of the fundamental extended modes from the flexible localized modes, as discussed above, protects the spin wave stiffness as well as the lifetime.

Spin pumping is the emission of spin currents from a magnetic material into metal contacts by the magnetization dynamics. The latter can be driven, for example, by

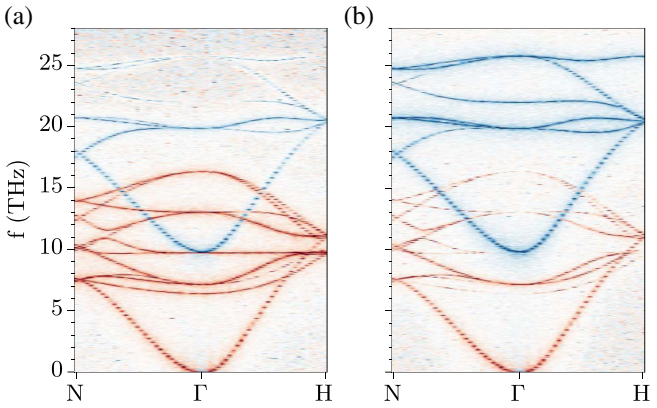

FIG. 3. Examples of the on-site correlations from different points in the unit cell: (a) FeA at $(0, 1/2, 0)$ and (b) FeA at $(1/2, 0, 0)$ in fractional coordinates.

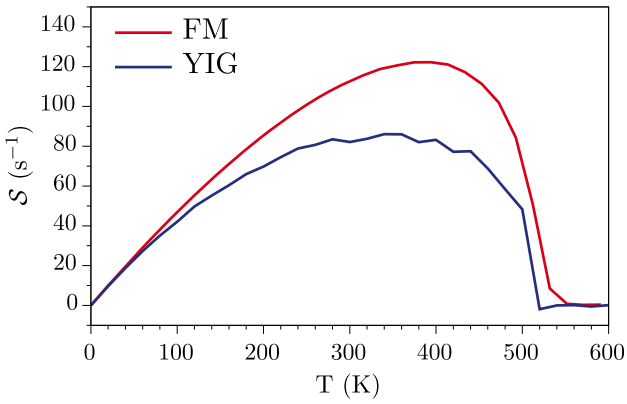

FIG. 4. Spin pumping [Eq. (6)] of YIG and a hypothetical ferromagnet into a metal contact as a function of temperature.

microwaves and ferromagnet resonance or by thermal excitations. In the presence of a temperature difference, the imbalance between thermal spin pumping and spin transfer torque from the metal causes net spin currents that can be converted into voltages by the inverse spin Hall effect, i.e., the spin Seebeck effect. Spin pumping and SSE are interface effects that are proportional to the spin-mixing interface conductance and equal-time and space spin correlation functions of the magnet at the interface [5]. When the interface correlations are identical to that in the bulk, i.e., are not perturbed by the presence of the interfaces (golden rule or tunneling approximation), our simulations provide direct access to the spin Seebeck effect except for a constant that contains the spin-mixing conductance, spin Hall angle, and temperature gradient. Our approach does not address surface spin wave states or spin-pumping-induced enhanced damping. For samples much thicker than the magnon relaxation lengths, thermal gradients induce magnon spin and heat transport in the bulk of the ferromagnet, which have been held responsible for, e.g., YIG layer thickness dependence of the SSE [6,10,14]. These effects are beyond the scope of the present study, however.

The spin-mixing conductance of an interface between a metal and a magnetic insulator with local moments is governed by the exchange integrals between the local moments and the conduction electrons [26]. The dc pumped spin current then reads

$$\langle \mathbf{I} \rangle_A = \frac{\hbar}{4\pi} \frac{\mathrm{Re} g^{\uparrow\downarrow}}{N_A} \sum_i^{N_A} \langle \mathbf{S}_i \times \dot{\mathbf{S}}_i \rangle, \tag{5}$$

where N_A are the number of moments at the interface A. Averaging over the (weak) dependence of the mixing conductance on the specific interface [26] and to leading order in the transverse dynamics, $\langle I_z \rangle = \hbar \mathrm{Re} g^{\uparrow\downarrow} \mathcal{S}/(4\pi)$, where the equal-time and space correlation function,

$$S = \frac{1}{N_c} \sum_i^{N_c} \langle \dot{S}_{y,i} S_{x,i} - \dot{S}_{x,i} S_{y,i} \rangle, \tag{6}$$

can be obtained either directly from the simulations or by integrating the spectral power functions discussed above over frequency and momenta. At equilibrium this current is exactly compensated by the thermal spin transfer torque-induced currents from the metal. The observed spin Seebeck voltage then reads, to leading order, $\Delta V_{\mathrm{SSE}} \sim \mathcal{S} \partial T$, where ∂T is the temperature gradient over the sample. We do not address the proportionality constant here. The correlation functions that govern electric spin injection, chemical potential-driven transport [12], which might be relevant for the spin Seebeck effect [27], as well as bulk magnonic transport that dominates the signal for thick ferromagnets, are the subject of ongoing study. In Fig. 4 we plot $\mathcal{S}$ as a function of temperature for YIG as well as for a hypothetical ferromagnet with parallel moments on a simple bcc lattice (FM) that is tuned to the same saturation magnetization and Curie temperature as YIG.

Both the ferrimagnet YIG and the FM show similar features. An increasing temperature initially increases spin pumping by enhanced thermal agitation. Close to the critical temperature spin pumping collapses to zero at T_C together with the net magnetization. The YIG spin pumping is maximized close to 300 K, i.e., far from the critical region of the phase transition. This is caused by the increasing thermal occupation of the high-frequency optical mode with opposite polarization, which plays a significant role above 300 K (see Fig. 2). A similar effect causes the low temperature sign change of the spin Seebeck signal in GdIG [13]. On the other hand, the thermal occupation of the optical modes actually enhances the net magnetization rather than decreasing it [3].

Uchida *et al.* [28] observed a power law $\Delta V_{\mathrm{SSE}} \sim (T_C - T)^3$ close to the Curie temperature T_C, while the magnetization scales $\sim (T_C - T)^{1/2}$ as expected from mean-field theory. Here we find the same critical exponent $(1/2)$ for both the magnetization and SSE effect, which can be rationalized in terms of the spin wave gap that is closed in proportion with the exchange field. The anomalous scaling found experimentally must be attributed to physical effects not related to the dynamic

susceptibility. A strong suppression of spin transport in the ferrimagnet by large thermal fluctuations is a possible explanation. On the other hand, the present spin Seebeck theory is based on the Landau-Lifshitz-Gilbert equation, which might not hold close to the phase transition. More study is needed to understand the spin Seebeck effect close to the critical regime.

IV. Conclusion.—We present atomistic simulations of the spin dynamics of the electrically insulating ferrimagnet yttrium iron garnet with application to the spin Seebeck effect. The calculations transcend previous theories by taking fully into account (i) the complicated crystal and ferrimagnetic structure and (ii) the nonlinearities caused by magnon-magnon interactions at elevated temperatures. We observe a remarkable resilience of the fundamental acoustic and optical modes with respect to thermal agitation, which is explained by their large dispersion and spatial isolation from numerous flexible modes with large heat capacity. At room temperature and above, the ferrimagnetic optical mode is significantly occupied. Its negative polarization leads to a suppression of thermal spin pumping and spin Seebeck effect. The critical exponent observed for the spin Seebeck effect [28] remains as yet unexplained.

This work was supported by JSPS KAKENHI Grants No. 25247056, No. 25220910, and No. 26103006 and by the Tohoku University Graduate Program in Spintronics. We thank Jiang Xiao and Hiroto Adachi for useful discussions.

[1] K. Uchida, J. Xiao, H. Adachi, J. Ohe, S. Takahashi, J. Ieda, T. Ota, Y. Kajiwara, H. Umezawa, H. Kawai, G. E. W. Bauer, S. Maekawa, and E. Saitoh, Nat. Mater. **9**, 894 (2010).
[2] G. E. W. Bauer, E. Saitoh, and B. J. van Wees, Nat. Mater. **11**, 391 (2012).
[3] V. Cherepanov, I. Kolokolov, and V. L'vov, Phys. Rep. **229**, 81 (1993).
[4] Y. Sun, Y.-Y. Song, H. Chang, M. Kabatek, M. Jantz, W. Schneider, M. Wu, H. Schultheiss, and A. Hoffmann, Appl. Phys. Lett. **101**, 152405 (2012).
[5] J. Xiao, G. E. W. Bauer, K.-c. Uchida, E. Saitoh, and S. Maekawa, Phys. Rev. B **81**, 214418 (2010).
[6] U. Ritzmann, D. Hinzke, and U. Nowak, Phys. Rev. B **89**, 024409 (2014).
[7] Y. Ohnuma, H. Adachi, E. Saitoh, and S. Maekawa, Phys. Rev. B **87**, 014423 (2013).
[8] S. O. Demokritov, B. Hillebrands, and A. N. Slavin, Phys. Rep. **348**, 441 (2001).
[9] J. S. Plant, J. Phys. C **10**, 4805 (1977).
[10] T. Kikkawa, K.-i. Uchida, S. Daimon, Z. Qiu, Y. Shiomi, and E. Saitoh, Phys. Rev. B **92**, 064413 (2015).
[11] H. Jin, S. R. Boona, Z. Yang, R. C. Myers, and J. P. Heremans, Phys. Rev. B **92**, 054436 (2015).
[12] L. J. Cornelissen, J. Liu, R. A. Duine, J. B. Youssef, and B. J. van Wees, Nat. Phys. **11**, 1022 (2015).
[13] S. Geprägs *et al.*, Nat. Commun. **7**, 10452 (2016).
[14] E.-J. Guo, J. Cramer, A. Kehlberger, C. A. Ferguson, D. A. MacLaren, G. Jakob, and M. Kläui, Phys. Rev. X **6**, 031012 (2016).
[15] S. R. Boona and J. P. Heremans, Phys. Rev. B **90**, 064421 (2014).
[16] S. R. Etesami, L. Chotorlishvili, and J. Berakdar, Appl. Phys. Lett. **107**, 132402 (2015).
[17] K. Uchida, M. Ishida, T. Kikkawa, A. Kirihara, T. Murakami, and E. Saitoh, J. Phys. Condens. Matter **26**, 389601 (2014).
[18] K. Uchida, H. Adachi, T. Kikkawa, A. Kirihara, M. Ishida, S. Yorozu, S. Maekawa, and E. Saitoh, Proc. IEEE **104**, 1946 (2016).
[19] D. Hinzke and U. Nowak, Comput. Phys. Commun. **121**, 334 (1999).
[20] E. E. Anderson, Phys. Rev. **134**, A1581 (1964).
[21] J. Oitmaa and T. Falk, J. Phys. Condens. Matter **21**, 124212 (2009).
[22] R. K. Wangsness, Phys. Rev. **91**, 1085 (1953).
[23] A. B. Harris, Phys. Rev. **132**, 2398 (1963).
[24] R. C. LeCraw and L. R. Walker, J. Appl. Phys. **32**, S167 (1961).
[25] R. Bastardis, U. Atxitia, O. Chubykalo-Fesenko, and H. Kachkachi, Phys. Rev. B **86**, 094415 (2012).
[26] X. Jia, K. Liu, K. Xia, and G. E. W. Bauer, Europhys. Lett. **96**, 17005 (2011).
[27] L. J. Cornelissen, K. J. H. Peters, G. E. W. Bauer, R. A. Duine, and B. J. van Wees, Phys. Rev. B **94**, 014412 (2016).
[28] K.-i. Uchida, T. Kikkawa, A. Miura, J. Shiomi, and E. Saitoh, Phys. Rev. X **4**, 041023 (2014).